5-1994

Validating Diurnal Climatology Logic of the MT-Clim Model Across a Climatic Gradient in Oregon

Joseph Marion Glassy
The University of Montana

Steven W. Running
University of Montana - Missoula

Recommended Citation

Glassy, J. M. and Running, S. W. (1994), Validating Diurnal Climatology Logic of the MT-CLIM Model Across a Climatic Gradient in Oregon. Ecological Applications, 4: 248–257. doi:10.2307/1941931

Ecological Applications, 4(2), 1994, pp. 248–257

VALIDATING DIURNAL CLIMATOLOGY LOGIC OF THE MT-CLIM MODEL ACROSS A CLIMATIC GRADIENT IN OREGON[1]

JOSEPH M. GLASSY AND STEVEN W. RUNNING
School of Forestry, University of Montana, Missoula, Montana 59812 USA

Abstract. This study tests diurnal climatology assumptions made in the MT-CLIM model by examining two microclimate variables driven by diurnal atmospheric dynamics: incident solar radiation (in kilojoules per square metre), and humidity, expressed as vapor pressure deficit, VPD (in kilopascals). The relative VPD humidity comparison was used to test our hypothesis that night minimum temperatures can function as a surrogate for dew-point temperatures. VPD was chosen as the humidity measure for these tests since plants are more directly sensitive to this measure than relative humidity. For the observed vs. estimated vapor pressure deficit models, we obtained coefficients of determination (R^2) ranging from 0.66 to 0.84. Incident solar radiation is calculated in the model using an algorithm that relates diurnal temperature amplitude to atmospheric transmissivity, coupled with a potential radiation model to compute diffuse and direct radiation. Correlations for incident solar radiation models indicate generally good agreement, with coefficients of determination ranging from $R^2 = 0.82$ to 0.89. These results suggest that MT-CLIM may be a useful way to provide the climatology that many ecological/hydrological models require, particularly for larger scale spatial modeling applications where precise meteorology may not be as important as a good general characterization of the regional climatology.

Key words: climate gradient of the Oregon Cascade Range; climatological parameters; diurnal climate modeling; Oregon transect; OTTER project; validating humidity measurements; validating solar radiation estimates; vapor pressure deficit vs. dew point.

INTRODUCTION

Climatology data requirements for ecological models

Climatology data play a critical role in regional- and global-scale ecosystem applications. In a review of climate information needs for ecological effects models, Peer (1990) describes 19 contemporary models, including biome-level, ecosystem process, species dynamics, individual-tree, and agricultural models, that all require basic meteorological data. Examples of such applications include hydroecologic models (Band and Wood 1988, Band et al. 1991), grassland models such as CENTURY (Parton et al. 1988), and forest and biome ecosystem process models (McMurtrie 1985, Running and Coughlan 1988, Running et al. 1989, Ågren et al. 1991, Running and Gower 1991). To exploit current remote sensing and geographical information system (GIS) approaches, many ecosystem models are evolving from one- to two-dimensional applications (Nemani et al. 1993), encouraging the development of better methods to generate climate surfaces. These modeling approaches span a large range of spatial and temporal scales, emphasizing the breadth of the climatological data requirement. Climatological parameters required by these models typically include air temperature, solar radiation, some measure of atmospheric humidity, precipitation, and, in some cases, wind speed and direction. Meteorology data sets available for ecological models are available in many diverse forms. Project-specific on-site data from portable meteorology stations is available, as well as more-localized archives such as the USDA Forest Service Remote Automated Weather Stations (RAWS) network (Warren and Vance 1981). Longer term meteorological data available includes archived historical weather data sets such as the Climatological Data Summaries maintained by the National Oceanic and Atmospheric Administration (NOAA), at the National Climatic Data Center (NCDC, Ashville, North Carolina), derived from U.S. National Weather Service (NWS) stations.

The quality of available meteorological data varies considerably, with problems ranging from missing values to erroneous data collected by poorly calibrated or faulty instruments. An equally serious problem is that in some cases variables of interest to ecological modelers, such as incident solar radiation and humidity, are simply not collected at all.

The MT-CLIM approach of using 24-h minimum temperature as a surrogate for dew point temperature attempts to address these deficiencies; the ability to further establish the strength and theoretical limitations of this relationship is important in light of the

[1] Manuscript received 24 August 1992; revised 25 March 1993; accepted 5 April 1993; final version received 1 May 1993.

relatively small fraction of established weather stations that collect humidity measurements of any kind. Running et al. (1987) estimated that the density of primary (NWS) stations recording humidity (as well as solar radiation) in any form was <1 station/100 000 km^2 throughout the western United States. The challenge for many ecosystem modelers is to match the qualitative and quantitative requirements of their models with the spatial and temporal scales of the various climatological data sources available. NWS Daily Climatological Summaries represent a dependable data source when good on-site weather data cannot be collected and NOAA weather satellite data are too coarse. However, the only variables routinely archived at both primary and secondary NWS sites are daily maximum and minimum air temperature (taken at 1.4 m above the ground) and precipitation. Dew point temperature measurements are taken, however, at some primary NWS sites, usually situated at major airports. Although originally intended to work using NWS station Daily Climatological Summary data, the MT-CLIM model may be driven using any weather station source that provides maximum and minimum temperatures and precipitation. Primary inputs to MT-CLIM include base station latitude, base station elevation, and site elevation, aspect, slope, albedo, atmospheric transmissivity, base and site precipitation isohyets, and temperature lapse rates (Table 1). Standard MT-CLIM outputs include daily microclimate values for air temperature (site temperature, and 24-h maximum and minimum temperatures, in degrees Celsius), incident solar radiation (400–2500 nm wavelengths, in kilojoules per square metre per day), relative humidity (in percent), and precipitation (in centimetres) in mountainous terrain.

Table 1. Example of MT-CLIM inputs (for NASA OTTER project MT-CLIM model validation): Cascade Head, Site 1.

Input example	Input choices and/or categories
S	SI (temperatures in °Celsius, precipitation in cm) or English (U.S. customary: temps. in °F, ppt. in inches) units? [S or E]
N	Dew point temperature supplied? [Yes or No]
1	Number of ppt. stations? [1 or 2] If 2 then use 2 isohyets below
N	Use threshold radiation? [Yes or No]
Y	Use yearday (day of year) in place of month-and-day? [Yes or No]
	Input variables*
208	No. of days
44.05	Latitude (degrees)
49.0	Site elevation (metres for SI or feet for English)
49.0	Base elevation (metres for SI or feet for English)
125.0	Site aspect, 0 to 360 degrees (0 = North; 180 = South)
10.0	Site slope (percent)
6.3	Site LAI (leaf area index, all-sided)
2.0	Site isohyet (precipitation)
2.0	Base isohyet station 1
0.0	Base isohyet station 2 (optional; see no. of ppt. stations, above)
1.0	Site east horizon (extent in degrees)
1.0	Site west horizon (extent in degrees)
0.16	Site albedo (0.2 = 20%)
0.60	TRANCF (sea level atmospheric transmissivity)
0.45	TEMPCF (temperature correction for sine approximation)
6.377	Temperature lapse rate (degrees/1000 km)
7.288	Lapse rate for maximum temperature (degrees/1000 km or ft)
3.644	Lapse rate for minimum temperature (degrees/1000 km or ft)
2.730	Dew point temperature lapse rate (degrees/1000 km or ft)

* No. of days is integer variable; all the rest are real numbers.

In response to the paucity of site-specific climatology data required for ecological process models, Running et al. (1987) devised a mountain microclimate simulator, the MT-CLIM model. MT-CLIM evolved from two earlier research models, H20TRANS and DAYTRANS (Running 1984), which evaluated the ecosystem-level significance of stomatal control mechanisms (transpiration and water stress) at hourly and daily time steps, respectively. MT-CLIM is composed of two types of climatology logic, the topographic climatology that spatially extrapolates meteorological conditions into complex terrain, and the diurnal climatology that derives additional meteorological information from the input data (Hungerford et al. 1989). In the topographic section of MT-CLIM daily data from primary NWS weather stations is extrapolated to nearby sites, adjusting for the differences in aspect, elevation, slope, and vegetation type between the site of interest and one or two base weather stations.

A key assumption in the development of the MT-CLIM logic, and one that distinguishes it from other meteorological models, is the concept of *operational environment* whereby important environmental variables are defined on the basis of plant physiology rather than only meteorologically (Mason and Lagenheim 1957, Waring et al. 1972, Waring and Schlesinger 1985). For example, day length can be defined in the MT-CLIM model in terms of the period when the light compensation point (70 W/m^2) for conifer needles is exceeded—the point at which conifer stomatal opening, transpiration, and positive net photosynthesis begins. In irregular or complex topography, this definition of day length may be 20% shorter than the full period from sunrise to sunset (Running et al. 1987). This threshold may be adjusted for other species as well.

The diurnal climatology in MT-CLIM generates two particularly problematic climatological parameters required by ecosystem process models—incident solar radiation (Running et al. 1987) and a humidity measure useful from a plant physiology standpoint (Grantz 1990). For this study our objective was to test key assumptions in the MT-CLIM model diurnal climatology logic by comparing incident solar radiation and relative humidities measured at five Oregon Transect

TABLE 2. Summary of key parameters of the OTTER (Oregon Transect Ecosystems Research) sites.

Site name	Meteorological station: Elevation (m)	Meteorological station: Location	Physiographic province	Mean leaf area index (LAI)
Cascade Head	49	44°3'0" N, 123°57'30" W	Western coast range	6.4
Waring's Woods	60	44°36'0" N, 123°16'0" W	Interior valley	5.3
Scio	335	44°40'30" N, 122°36'40" W	Low elev. west Cascades	8.6
Santiam Pass	1500	44°25'20" N, 121°50'20" W	High Cascades summit	2.8
Metolius	1027	44°25'0" N, 121°40'0" W	Eastern high Cascades	2.0

Ecosystem Research (OTTER) sites against MT-CLIM estimations of these parameters.

METHODS

This study was conducted as part of the National Aeronautics and Space Administration (NASA) Oregon Transect Ecosystem Research (OTTER) project (Peterson and Waring 1994 [this issue]). The OTTER project includes six primary sites along a 250-km east–west transect through central Oregon at 44° north latitude, with elevations ranging from sea level to 1500 m. A timely opportunity to further validate basic assumptions in the MT-CLIM model was presented since each of the five main OTTER sites was equipped with a portable weather station (Campbell Scientific, Logan, Utah, USA). Incident solar radiation was recorded at each OTTER site using a LI-COR LI220S pyranometer, sensitive to radiation at 400–2500 nm wavelengths. Relative humidity (RH) was recorded using a PCRC-55 humidity sensor (Campbell Scientific). At each OTTER site during 1989 and 1990 hourly measurements of 13 meteorological variables were collected, including minimum and maximum temperature, relative humidity, and incident solar radiation; the daily data set we used was prepared from this hourly data set. In this data set daylight is defined as the full period from sunrise to sunset. Key site parameters for the five OTTER sites used in this study are presented in Table 2. Only sites with meteorology stations were used for this study; the easternmost site (Juniper) relied on the meteorology station at the Metolius site. For a more complete description of OTTER site characteristics, refer to Runyon et al. (1994) and Goward et al. (1994) [this issue].

The observed data for this study were obtained from the Forest Science Data Base (FSDB) maintained by Oregon State University as part of the Long Term Ecological Research (LTER) data holdings. Daily observation data from 1989 and 1990 were extracted from the daily meteorological data set. Our goal was to assemble as close to a full annual data sequence as possible, both to ensure an adequate sample size and to reveal any trends in the data that might have been phenologically driven. Several date ranges of observed data were excluded for four of the five sites (all sites but Santiam Pass) due to known calibration problems with the RH sensors. Table 3 contains a description of the date ranges and total number of days used in this analysis. Daylight is defined within the LTER database as the time from sunrise to sunset, and so the model was set to match this definition of day length. The site variables used were 24-h minimum and maximum air temperature (in degrees Celsius), daylight average relative humidity (in percent), total incident solar radiation (in kilojoules per square metre per day), and precipitation (in millimetres per day).

Humidity and vapor pressure deficit

There are several common ways of expressing humidity, including vapor density, relative humidity (RH), and vapor pressure deficit (VPD). Vapor density is simply the mass of water vapor in a unit volume of air and is also known as absolute humidity (Oke 1987). The most commonly collected humidity measure, relative humidity, is defined as the actual moisture content of a parcel of air as a percentage of that contained in the same volume of saturated air at the same temperature (Barry and Chorley 1987). Dew-point temperature, another index of humidity, is the temperature at which saturation occurs if air is cooled at constant pressure without addition or removal of vapor (Barry and Chorley 1987). The relative humidity varies inversely with temperature during the day, tending to be lower in the early afternoon and higher at night. When the RH is 100% the air temperature and dew-point temperature are equal. Vapor pressure is a measure of

TABLE 3. Seasonal distribution of date ranges and total number of days used in this analysis, by site (Oregon, USA).

Site	1989 days	1990 days	Total days
Cascade Head	7 Jun–31 Dec	1 Jan–31 May	359
Waring's Woods	28 May–31 Dec	1 Jan–31 Mar	308
Scio	28 May–31 Dec	1 Jan–31 Mar	308
Santiam Pass	26 Jun–5 Nov	9 May–25 Nov	334
Metolius	5 Jun–31 Dec	1 Jan–31 Mar	299

the partial pressure exerted by water vapor molecules in the air (Oke 1987). The saturation vapor pressure deficit of an air parcel is the difference between the saturation vapor pressure and the actual vapor pressure. In an ecological context, VPD may be the most useful measure of humidity, as it represents a measure of the *drying power* of air, playing an important part in determining the relative rates of transpiration in plants (Monteith and Unsworth 1990).

To test the MT-CLIM diurnal humidity logic, VPD was chosen as a humidity measure as opposed to RH since plants physiologically respond more readily to fluctuations in VPD than to changes in RH (Grantz 1990). Ecological process variables dependent on VPD include evapotranspiration (ET), stomatal conductance, photosynthesis (PSN) dynamics, and plant water relations. VPD also plays a key role in stomatal conductances (Gates 1980, Jarvis and Morison 1981, Friend 1991) and in plant water flow resistances (Hunt et al. 1991). Running et al. (1987) reported an R^2 coefficient of 0.85 for the relationship between dew point temperature and 24-h minimum temperature for three stands in the Lubrecht Experimental Forest in western Montana; in the same study, he also reported R^2 coefficients for relative humidity algorithms of 0.59, 0.43, and 0.60 for three western Montana drainages.

Measuring humidity dependably over time has always been a challenge to meteorologists, due to the calibration, reliability, and longevity problems that humidity instruments are subject to. When a given set of meteorological data is obtained, it is helpful to know the type of humidity-sensing instrument used; unfortunately, this information is not always available in the data set documentation. In general, laboratory quality dew point hygrometers are more accurate (Oke 1987). Unfortunately their expense, power requirements, and the necessity for periodic calibration tends to limit their use to primary NWS (National Weather Service) weather stations. The less expensive humidity instruments are based on chemical or electrical sensors where the humidity is measured on the basis of changes in chemical substrate or electrical properties due to moisture absorption; these types tend to be the most prone to degradation problems. In the OTTER study, for example, within several months of initial installation the digital RH sensors at all sites except the Santiam site exhibited a premature signal degradation, seriously compromising the data's usefulness (Goward et al. 1994 [this issue]). The degradation problem was diagnosed in terms of RH trends at the affected sites increasingly departing from expected diurnal recovery levels. Field conditions apparently caused some physical loss of the RH sensor substrate over time, resulting in a systematic reduction in sensitivity and signal gain. This problem necessitated additional screening and verification of the measured relative humidity data from all sites but the Santiam Pass site.

For this analysis we used daylight average relative

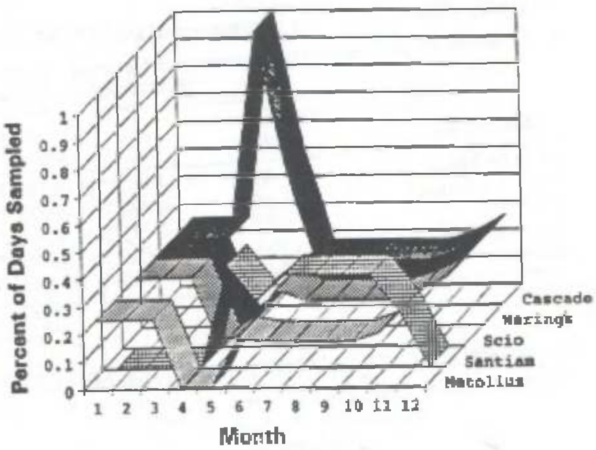

FIG. 1. Frequencies of days sampled by month for two sample years (1989 and 1990), by OTTER site.

humidity; only contiguously sequenced days with no missing values for temperature, radiation, or precipitation qualified for inclusion in the analysis data set. We specifically excluded observations where the day fell within a time period where the RH sensor for the site was known to have degraded. Adequate sample sizes were thus obtained by using qualifying data from both 1989 and 1990 (Fig. 1); as a result of these exclusions, contiguous 365-d sequences for each site were not possible.

The MT-CLIM model estimates site relative humidity and vapor pressure deficits using a scheme whereby dew-point temperature is used in Murray's (1967) formulation:

$$\mathrm{esd} = 0.61078 \cdot e^{\left[\frac{17.269 \cdot T_{\mathrm{Site}}}{237.3 + T_{\mathrm{Site}}}\right]}, \qquad (1)$$

where esd is saturated vapor pressure (in kilopascals) and T_{Site} is average daylight site temperature (in degrees Celsius);

$$\mathrm{es} = 0.61078 \cdot e^{\left[\frac{17.269 \cdot T_{\mathrm{Dew}}}{237.3 + T_{\mathrm{Dew}}}\right]}, \qquad (2)$$

where es is ambient vapor pressure (in kilopascals) and T_{Dew} is dew-point temperature (in degrees Celsius); and

$$\mathrm{RH}_{\mathrm{Site}} = \left[\frac{\mathrm{es}}{\mathrm{esd}}\right] \cdot 100, \qquad (3)$$

where $\mathrm{RH}_{\mathrm{Site}}$ is the daylight average site relative humidity (in percent).

Two forms of these equations were used to produce the "observed" VPD vs. the "estimated" VPD, differing only in the way that ambient vapor pressure (es) was computed. To produce the observed VPD, saturated vapor pressure (esd) was computed exactly as shown in Eq. 1 and the site ambient vapor pressure was computed using a simple algebraic transform of the RH equation (Eq. 3)

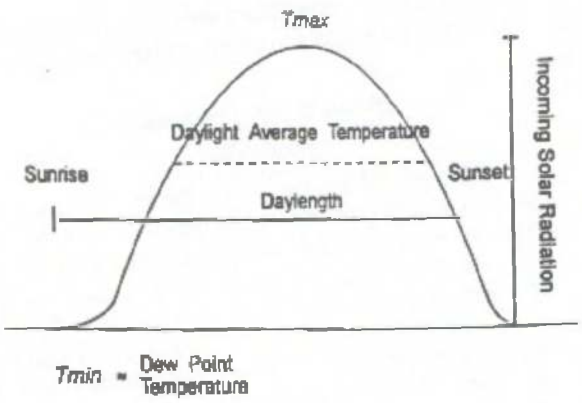

FIG. 2. Diagram of MT-CLIM diurnal logic illustrating the relationship of diurnal minimum and maximum temperature, incoming solar radiation, and the truncated period defining daylight average temperature.

$$es = \frac{RH_{Obs}}{100} \cdot esd, \qquad (4)$$

where RH_{Obs} is the measured daylight average RH (in percent) at the base station.

Vapor pressure deficit is defined simply as the difference between saturated and ambient vapor pressures, VPD = esd − es (Oke 1987, Monteith and Unsworth 1990). To compute the "estimated" VPD for each site, ambient vapor pressure (es) was computed using Eq. 2, substituting the night minimum temperature for dew point temperature. Saturated vapor pressure (esd) was computed for the estimated VPD in the usual way as in Eq. 1.

Incident solar radiation

The method MT-CLIM uses for computing solar radiation on the site is adapted from the methods of Bristow and Campbell (1984) and is driven solely by diurnal temperature amplitude, freeing it from the requirement of historically questionable cloud-cover estimates. Our hypothesis that diurnal air-temperature amplitude (Fig. 2) relates directly to incident solar radiation loading assumes a horizontally stable atmosphere over the region of interest, with no significant advective exchange. To the extent that stable conditions dominate, the model should perform fairly well. One implication of this diurnal temperature approach is that the performance of our model in estimating solar radiation is critically dependent on the many ways in which air masses may be horizontally modified; an air mass may be heated from below either by passing from a cold to a warm surface or by solar heating of the ground over which the air is located (Barry and Chorley 1987). When significant horizontal air movement does occur, the differing temperatures and energy exchange properties of these masses can disproportionately control air temperatures and thus mask or override the more direct influence of solar radiation, weakening the model's performance. Topographically driven phenomena such as cold air drainages, frost pockets, and physiographic formations that generate or amplify local winds can exert a similar effect. Synoptic-scale frontal systems, local temperature inversions, and extremely mesic environments where latent heat exchange dampens the diurnal temperature amplitude present additional meteorological phenomena that the Bristow and Campbell (1984) based approach cannot accommodate well.

The daily 24-h average incident solar radiation values measured at each of the five OTTER sites were compared directly against the MT-CLIM estimated values, using the total incident solar radiation (24 h) as the observed data. Incident solar radiation at each site was computed in MT-CLIM using the algorithms documented in Running et al. (1987) requiring only observed daily minimum and maximum temperatures. Clear sky transmissivity was first computed, assuming a value of 0.60 for mean sea level, increasing by 0.008 m^{-1} with elevation. Final atmospheric transmissivity was then computed as a function of diurnal temperature amplitude, following the method of Bristow and Campbell (1984). The logic behind this relationship is that the total transmittance for a given day includes both direct and diffuse components incident on a horizontal surface, and therefore integrates the atmospheric attenuation coefficients implicitly (Bristow and Campbell 1984). Next, a potential radiation model adapted from Garnier and Ohmura (1968) and Swift (1976) was used to calculate direct and diffuse solar radiation, adjusting for slope and aspect and truncating the direct beam solar irradiance by the east and west horizon of the site. The final estimate of incoming solar radiation to the site was then computed as the above-atmosphere radiation reduced by the atmospheric transmittance.

The diurnal temperature range, ΔT, is calculated by the equation:

$$\Delta T_{YD} = T_{maxYD} - \frac{[T_{minYD} + T_{(minYD+1)}]}{2}, \qquad (5)$$

where YD is the yearday index (day of year = 1 ... 365), T_{maxYD} is the daily maximum temperature (in degrees Celsius), T_{minYD} is the daily minimum temperature (in degrees Celsius), and ΔT_{YD} is range in daily temperature extremes.

The relationship between diurnal temperature amplitude and atmospheric transmittance is calculated using the Bristow and Campbell (1984) formulation:

$$\tau_t = A[1 - e^{(-B\Delta T^C)}], \qquad (6)$$

where τ_t is the daily total transmittance, ΔT is the daily range of air temperature, and A is the maximum clear sky transmittance, B (−0.0030), and C (2.4) are empirical constants that determine how soon τ_t is achieved as ΔT increases. The B and C constants represent the partitioning of energy characteristic of the modeled site. Although these have historically been fixed at the above values for all sites, future revisions of MT-CLIM should incorporate a better strategy for determining the seasonal site characteristics driving this relationship.

The equation used to compute potential incoming radiation is:

$$Q_s = \mathrm{Is}_s + D_s, \tag{7}$$

where Q_s is the total incoming radiation on a slope (in kilojoules per square metre) at the Earth's surface, Is_s is the direct beam radiation on a slope at the Earth's surface, and D_s is the diffuse radiation at the surface; the direct beam radiation Is_s at the surface is calculated by:

$$\mathrm{Is}_s = \cos\phi(R_o N \cdot \tau_t^{(\mathrm{AM})}) \tag{8}$$

where R_o is the solar constant (in kilowatts per square metre) above the atmosphere as a monthly average, N is the time interval for calculation in seconds, τ_t is the daily total transmittance from Eq. 6, and AM is the optical air mass, calculated using the equation:

$$\mathrm{AM} = \left[\frac{1.0}{\cos\Theta}\right] + 1.0 \cdot 10^{-7}, \tag{9}$$

where $\cos\Theta$ is the cosine of the zenith angle (see Running et al. [1987] for more details).

Simulations and analysis

Two sets of MT-CLIM simulations were run to generate observed and predicted values using versions of MT-CLIM in which the humidity algorithms were modified as discussed above. The observed solar radiation values (as 24-h averages) used were the original values measured at each of the five sites with the LI220S pyranometer mounted on portable weather stations. The first set of simulations produced the observed VPD values for each of the five sites, and the second set of simulations produced the estimated VPD values and estimated incident solar radiation values for each of the five sites.

Several statistics were used to evaluate algorithm performance, including the coefficient of determination (R^2), the beta and y-intercept linear regression coefficients, and the root mean square error, RMSE. The RMSE provides an indication of curve fit accuracy, with observed values close to estimated values resulting in a lower RMSE. The RMSE is a conservative error measure that tends to penalize large individual errors heavily (Reicosky et al. 1989). Standard two-tailed hypothesis tests of the model beta (β_1) coefficients (H_0: $\beta_1 = 0$, H_A: $\beta_1 \neq 0$) and y intercepts (using the same two-tailed tests) were employed to further investigate the strength of the fitted models. Lastly, F statistic and t statistic probability values were calculated to evaluate the overall quality of the linear regression models. All statistics were computed using the SPSS/PC+ statistical software package (Norusis 1988).

Results and Discussion

Humidity

Coefficients of determination for the observed vs. predicted VPD (vapor pressure deficit) models ranged from $R^2 = 0.66$ to 0.84, with F statistics significant at the .001 probability level, with three of the five sites R^2 coefficients >0.80. This suggests that the VPD approach yields acceptable results overall, particularly in light of a pooled site VPD R^2 of 0.72. An examination of normal P–P plots indicated no serious departures from normality, and plots of casewise standardized residuals vs. fitted values indicated no obvious patterns in error trends. There was a slight clustering trend in R^2 coefficients, with the wetter, more productive sites (Cascade Head and Scio) having the lower correlations ($R^2 = 0.66$ and 0.68, respectively) and the other sites' R^2 values ranging from 0.80 to 0.83 (see Table 4). The distribution of point values for most sites was slightly skewed, due in part to a slightly asymmetric sampling distribution seasonally (Fig. 1). Regression model slopes for the VPD models ranged from a low slope of 0.72 at the middle elevation, productive Scio site to a high slope of 1.5 at the cool, moist Cascade Head site (Fig. 3). VPD regression y intercepts ranged from 0.13 to 0.31 kPa, which in conjunction with the positive slopes contributed to a slight trend towards overprediction. The Santiam Pass VPD regression model, where observed data did not require screening, may represent a useful average case of MT-CLIM's humidity performance; the regression slope for this site was 1.001 with a y intercept of 0.31 kPa (Fig. 4). In general, MT-CLIM somewhat overpredicted VPD across all sites except Scio.

In this study where the emphasis was on testing the diurnal logic of MT-CLIM, the "base station" site characteristics were identical to the "extrapolated" sites; corrections for changes in aspect, elevation, or slope were therefore not required. When the extrapolated site does markedly differ in aspect, elevation, and slope from the base station site, it is possible for the MT-CLIM model to slightly over- or underestimate air temperatures at the target site, due to the way the algorithms extrapolate the base station daily T_{max} and T_{min} temperatures to the new site characteristics. Such errors in estimated air temperature, if present, would naturally affect the VPD estimates. For process models depending on these humidity estimates, this would likely result in somewhat higher transpiration rates and altered soil-water dynamics. Limited availability of dependable humidity or dew-point temperature data for ecosystem research applications appears to justify further efforts to strengthen the MT-CLIM approach. Better correction logic, however, still needs to be developed to accommodate the meteorological conditions

TABLE 4. Solar radiation and VPD analysis summary.*

Site	R^2	SE y'	RMSE	Regression model	N
Incident solar radiation relationships (radiation in kJ/m²)					
Cascade Head	0.83	2878.5	3267.5	$y = 0.792(x) - 657.4$	359
Waring's Woods	0.89	3033.9	997.9	$y = 1.054(x) - 1499.8$	308
Scio	0.88	2736.5	4498.3	$y = 0.806(x) - 1763.8$	308
Santiam Pass	0.84	3881.4	1619.4	$y = 1.048(x) - 2302.1$	334
Metolius	0.84	4134.6	1667.5	$y = 1.010(x) - 1804.8$	299
All sites pooled	0.85	3691.9	2733.0	$y = 0.959(x) - 1678.6$	1608
Vapor pressure deficit relationships (VPD in mb)					
Cascade Head	0.68	0.192	0.38	$y = 1.537(x) + 0.2706$	359
Waring's Woods	0.82	0.242	0.43	$y = 1.293(x) + 0.2953$	308
Scio	0.66	0.205	0.11	$y = 0.727(x) + 0.1345$	308
Santiam Pass	0.84	0.213	0.33	$y = 1.001(x) + 0.3143$	334
Metolius	0.81	0.236	0.38	$y = 1.409(x) + 0.1671$	299
All sites pooled	0.72	0.269	0.364	$y = 1.104(x) + 0.2634$	1608

* N is the no. of data points; R^2 is the coefficient of determination for the least-squares model fits; RMSE is the root mean square error; SE y' is standard error of the estimate (for fitted y values). t statistic significant at $\leq .001$ for all model beta coefficients and y intercepts; F statistic significant at $\leq .001$ for all regression models.

described earlier that MT-CLIM currently doesn't handle well.

As a wider geographic test of the basic relationship between dew-point temperature and 24-h minimum temperature, we fitted linear regression models for daily weather data from six National Weather Service sites across the continental United States equipped with higher quality dew-point hygrometers. An annual sequence of 365 d for 1984 was used for each of the following sites: Fairbanks, Alaska; Seattle, Washington; Knoxville, Tennessee; Madison, Wisconsin; Tucson, Arizona; and Jacksonville, Florida. R^2 values for these regression models ranged from 0.83 to 0.96, with the exception of the drier Tucson site, whose R^2 was 0.55. Model slopes ranged from 0.80 to 1.02, and y intercepts ranged from -6.95 to 1.05°C. While acknowledging the climatological limitations of these relationships in drier environments, we believe these correlations suggest the basic soundness of the dew point–minimum temperature relationship. Particularly in more arid environments with lower absolute humidities, lower leaf area index (LAI) levels, and greater clear-sky re-radiation, the dew-point temperature may often be lower than the reported 24-h minimum temperature, and thus may never be reached (Lee 1978, Monteith and Unsworth 1990). A positive correlation between dew-point and daily minimum temperature also depends in part on dew point remaining fairly constant throughout the day; significant changes in air mass moisture from advective exchange are expected to alter this basic relationship. We generally feel, however, that the correlation between dew-point temperature and 24-h minimum temperature is strong enough on average to be of use in many ecological modeling applications, particularly since RH (relative humidity) sensors are so undependable. The dew-point temperature–24-h minimum temperature correlation we ob-

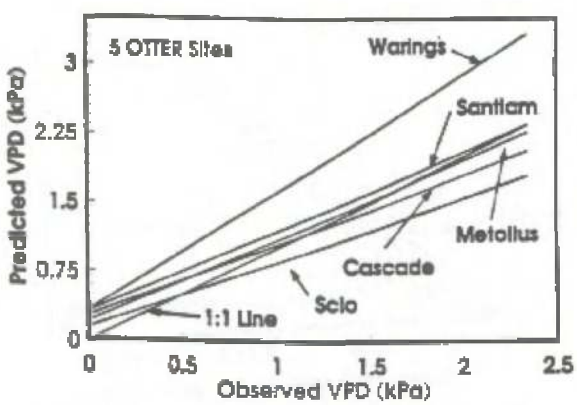

FIG. 3. Comparative plot of vapor pressure deficit (VPD) regression lines for the five sites, illustrating the ranking of the regression slopes across the site gradient.

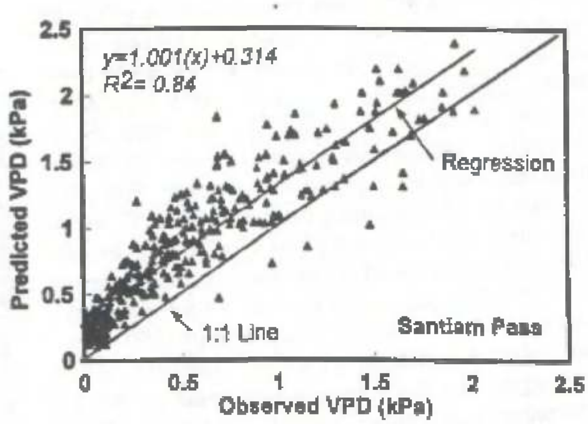

FIG. 4. Scatterplot and regression line of the vapor pressure deficit (VPD) model for the Santiam Pass (Oregon) OTTER site using 1989 and 1990 LTER (Long Term Ecological Research) data. This regression model provides a representative example of average humidity performance since data from this site did not require screening.

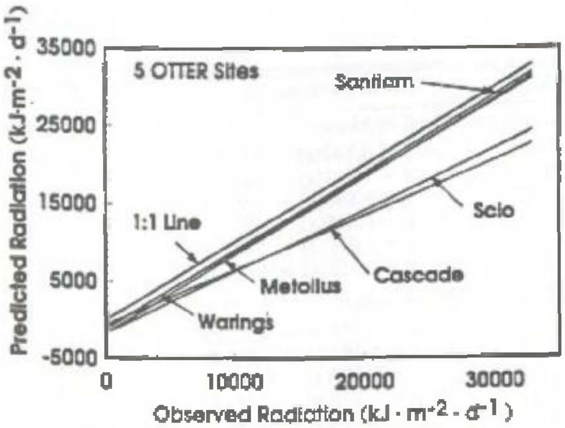

FIG. 5. Comparative plot of incident solar regression lines for the five sites, illustrating the division of the lines into two basic groups.

served may be particularly useful for studies employing larger spatial and temporal scales, where the higher variance in diurnal humidity and temperatures may be smoothed out at larger scales.

Incident solar radiation

Correlations between predicted and observed incident solar radiation were generally consistent and high, ranging from 0.83 to 0.89 (Table 4), with F statistics significant at the .001 level for all regression models. Regression slope t statistics testing the two-tailed null hypotheses, H_0, that the beta coefficient equals 0 and that the y intercept equals 0 were all significant at the .001 level, indicating the null hypotheses should be rejected. The regression model beta coefficients for the sites tended to split into two groups, with Cascade Head and Scio beta coefficients at 0.79 and 0.80, respectively, and Metolius, Santiam Pass, and Warings Woods beta coefficients ranging from 1.01 to 1.05 (Fig. 5). This division did not seem to occur on a clear environmental gradient, and could therefore relate to local advection conditions, inversions, or random error from sampling noise. Model y intercept values were all negative, ranging from -657 kJ/m^2 at the Cascade Head site to -2352 kJ/m^2 for Santiam Pass; the y intercept two-tailed t statistical significance for all radiation regression models was .01 or better. This statistic tests the H_0 that the y intercept equals 0, vs. a H_A that the y intercept is not equal to 0. The scatterplot and regression line fitted for the incident solar regression (Waring's Woods site, Fig. 6) shows a dense point cluster around the lower radiation range ($\approx$1000–4000 kJ$\cdot$m$^{-2}\cdot$d^{-1}) with a fairly balanced cluster for higher values; again, the slight pattern here could be due to the presence of advection effects on sampled days. Root mean square error (RMSE) values for the incident solar relationships ranged from 997.0 kJ to 4498.0 kJ, with no apparent trend following the west–east transect gradient. Normal P–P plots for the radiation data showed no serious departures from normality, and casewise plots of standardized radiation model residuals vs. fitted values indicated no obvious patterns in error trends. As a check on how regression VPD and solar radiation residuals might covary, plots of VPD residuals vs. incident solar residuals were examined, both by site and by pooling data for all sites; no trends were observed for either type of plot. Overall, the consistent strength of the incident solar relationships suggests this method may be sufficiently robust under a typical range of meteorological conditions (M. G. Ryan, *personal communication*; J. Barron, *personal communication*).

CONCLUSIONS

The comparisons made here between observed and estimated radiation and humidity suggest that MT-CLIM can provide acceptable climatology inputs for many hydrologic and ecosystem models. This approach may prove particularly useful for coarser spatial-scale applications where absolute precision at higher spatial resolutions may not be as important as an adequate characterization of incident solar radiation, diurnal temperature variations, and humidity dynamics over larger regions. The problems with humidity instruments and the current lack of incident solar radiation data archived daily at National Weather Service (NWS) weather stations further supports the value of this approach. Two projects in the International Geosphere-Biosphere Program have identified the need for a "weather generator" that takes standard climatological data and estimates additional meteorological variables needed by ecological research. The GCTE (Global Change and Terrestrial Ecosystems), and the BAHC (Biospheric Aspects of the Hydrologic Cycle) projects are collaborating on developing these weather generator tools to improve both the temporal and spatial utility of climate data sets for ecological studies. We think that MT-CLIM may be a useful precursor model for this new work.

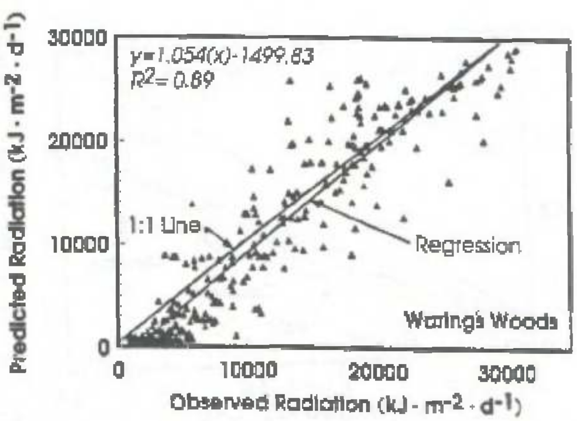

FIG. 6. Scatterplot and regression line of the incident solar radiation model for the Waring's Woods (Corvallis, Oregon) OTTER site using 1989 and 1990 LTER data.

Aside from problems relating to the quality of input data, a revision of MT-CLIM should attempt to redress current limitations in the model extrapolation logic. Areas needing improvement include a provision for adjusting between sites with significantly different air mass moisture properties (e.g., low coastal vs. dry inland sites), and a better way to generally address horizontal advection influences. Addressing estimation error due to cold air drainage influences and other topographically driven phenomena would probably require more radical changes, extending the model from a one-dimensional point model to a two-dimensional spatially connected model. The term "spatially connected" as used here implies that the modeled point may be influenced, at the very least, by selected landscape characteristics of neighboring areas. If a more spatially connected approach was pursued, a more explicit treatment of the topography directly influencing the modeled site could then be taken into account. The question of landscape scale becomes a critical one here, as a treatment of micro-topography effects would likely differ from drainage-level or even mesoscale topographic influences. An additional but related challenge involves how valley and katabatic diurnal wind patterns might be treated in the model, if at all. Relative to the current more simplistic MT-CLIM logic, such approaches would likely involve some conscious trade-offs in model complexity and parameterization.

The VPD relationships observed in this study, particularly for the Cascade Head and Scio sites, were not as conclusive as we would have liked, probably due to a combination of meteorological conditions not handled well in MT-CLIM as well as the selection of observed days (Fig. 2 and Table 3). Nonetheless, they may be sufficiently useful for larger scale modeling efforts for the reasons indicated above for solar radiation. Quality and maintenance of humidity sensors routinely used in the field were also important issues this study confronted, suggesting that it may be more advantageous to extrapolate from more distant but arguably higher quality NWS primary weather stations using dew-point hygrometers than to rely on less expensive and more problematic electro-chemical based RH instruments with shorter operational life-spans.

Acknowledgments

This research was supported by grants NAGW-252 and NAGW 1892 of the National Aeronautics and Space Administration, Earth Sciences and Applications Division, and by NSF grant BSR-8919649 to Steven W. Running. Special thanks go to John Runyon of Oregon State University for providing assistance with the observed climate database, and to Lars Pierce of the University of Montana School of Forestry NTSG for assistance and overall guidance in the analysis.

Literature Cited

Ågren, G. I., R. E. McMurtrie, W. J. Parton, J. Pastor, and H. H. Shugart. 1991. State-of-the-art of models of production–decomposition linkages in conifer and grassland ecosystems. Ecological Applications 1:118–138.

Band, L. E., D. L. Peterson, S. R. Running, J. Coughlan, R. Lammers, J. Dungan, and R. R. Nemani. 1991. Forest ecosystem processes at the watershed scale: basic for distributed simulation. Ecological Modelling 56:171–196.

Band, L. E., and E. F. Wood. 1988. Strategies for large scale, distributed hydrologic simulation. Journal of Applied Mathematics and Computation 27:23–37.

Barry, R. G., and R. J. Chorley. 1987. Atmosphere, weather and climate. Fifth edition. Routledge, London, England.

Bristow, K. L., and G. S. Campbell. 1984. On the relationship between incoming solar radiation and daily maximum and minimum temperature. Agricultural Forest Meteorology 31:159–166.

Friend, A. D. 1991. Use of a model of photosynthesis and leaf microenvironment to predict optimal stomatal conductance and leaf nitrogen partitioning. Plant Cell and Environment 14:895–905.

Garnier, B. J., and A. Ohmura. 1968. A method of calculating the direct shortwave radiation income on slopes. Journal of Applied Meteorology 7:796–800.

Gates, D. M. 1980. Biophysical ecology. Springer-Verlag, New York, New York, USA.

Goward, S. N., R. H. Waring, D. G. Dye, and J. Yang. 1994. Ecological remote sensing at OTTER: satellite macroscale observations. Ecological Applications 4:322–343.

Grantz, D. A. 1990. Plant response to atmospheric humidity. Plant Cell and Environment 13:667–679.

Hungerford, R. D., R. R. Nemani, S. W. Running, and J. C. Coughlan. 1989. MTCLIM: a mountain microclimate simulation model. Research Paper INT-414. USDA Forest Service, Intermountain Research Station, Ogden, Utah, USA.

Hunt, E. R., Jr., S. W. Running, and C. A. Federer. 1991. Extrapolating plant water flow resistances and capacitances to regional scales. Agricultural Forest Meteorology 54:169–195.

Jarvis, P. G., and J. I. L. Morison. 1981. The control of transpiration and photosynthesis by the stomata. Pages 247–278 *in* P. G. Jarvis and T. A. Mansfield, editors. Stomatal physiology. Cambridge University Press, Cambridge, England.

Lee, R. 1978. Forest microclimatology. Columbia University Press, New York, New York, USA.

Mason, H. L., and J. H. Langenheim. 1957. Language analysis and the concept of environment. Ecology 38:325–339.

McMurtrie, R. E. 1985. Forest productivity in relation to carbon partitioning and nutrient cycling: a mathematical model. Pages 194–207 *in* M. G. R. Cannell and J. E. Jackson, editors. Attributes of trees as crop plants. Institute of Terrestrial Ecology, Abbots Ripton, Huntington, England.

Monteith, J. L., and M. H. Unsworth. 1990. Principles of environmental physics. Edward Arnold, London, England.

Murray, F. W. 1967. On the computation of saturation vapor pressure. Journal of Applied Meteorology 6:203–204.

Nemani, R. R., S. W. Running, L. Band, and D. Peterson. 1993. Regional hydro ecological simulation system: an illustration of the integration of ecosystem models in a GIS. Pages 296–304 *in* M. Goodchild, B. Banks, and L. Steyert, editors. Integrating GIS and environmental modelling. Oxford, London, England.

Norusis, M. J. 1988. SPSS/PC+ version 3.0 update manual. SPSS, Chicago, Illinois, USA.

Oke, T. R. 1987. Boundary layer climates. Second edition. Routledge, New York, New York, USA.

Parton, W. J., J. W. B. Stewart, and C. V. Cole. 1988. Dynamics of C, N, P, and S in grassland soils: a model. Biogeochemistry 5:109–131.

Peer, R. L. 1990. An overview of climate information needs for ecological effects models. Contract number 68-02-4288. Atmospheric Sciences Modelling Division, Air Resources

Laboratory, National Oceanic and Atmospheric Administration, Research Triangle Park, North Carolina, USA.

Peterson, D. L., and R. H. Waring. 1994. Overview of the Oregon Transect Ecosystem Research project. Ecological Applications 4:211–225.

Reicosky, D. C., L. J. Winkelman, J. M. Baker, and D. G. Baker. 1989. Accuracy of hourly air temperatures calculated from daily minima and maxima. Agricultural and Forest Meteorology 46:193–209.

Running, S. W. 1984. Documentation and preliminary validation of H2OTRANS and DAYTRANS, two models for predicting transpiration and water stress in western coniferous forests. Research Paper RM-252. USDA Forest Service, Rocky Mountain Forest and Range Experiment Station, Fort Collins, Colorado, USA.

Running, S. W., and J. C. Coughlan. 1988. FOREST-BGC, a general model of forest ecosystem processes for regional applications. I. Hydrologic balance, canopy gas exchange and primary production processes. Ecological Modelling 42:125–154.

Running, S. W., and S. T. Gower. 1991. FOREST-BGC, a general model of forest ecosystem processes for regional applications. II. Dynamic carbon allocation and nitrogen budgets. Tree Physiology 9:147–160.

Running, S. W., R. R. Nemani, and R. D. Hungerford. 1987. Extrapolation of synoptic meteorological data in mountainous terrain and its use for simulating forest evapotranspiration and photosynthesis. Canadian Journal of Forest Research 17:472–483.

Running, S. W., R. R. Nemani, D. L. Peterson, L. E. Band, D. F. Potts, L. L. Pierce, and M. A. Spanner. 1989. Mapping regional forest evapotranspiration and photosynthesis and coupling satellite data with ecosystem simulation. Ecology 70:1090–1101.

Runyon, J., R. H. Waring, S. N. Goward, and J. M. Welles. 1994. Environmental limits on net primary production and light-use efficiency across the Oregon transect. Ecological Applications 4:226–237.

Swift, L. W., Jr. 1976. Algorithm for solar radiation on mountain slopes. Water Resources Research 12:108–112.

Warren, J. R., and D. L. Vance. 1981. Remote automatic weather station for resource and fire management agencies. General Technical Report INT-116. USDA Forest Service, Intermountain Research Station, Ogden, Utah, USA.

Waring, R. H., K. L. Reed, and W. H. Emmingham. 1972. An environmental grid for classifying coniferous forest ecosystems. Pages 1-26–13-26 *in* Proceedings: Research on Coniferous Forest Ecosystems—A Symposium. Bellingham, Washington, 23–24 March 1972. Pacific Northwest Forest and Range Experimental Station, USDA Forest Service, Portland, Oregon, USA.

Waring, R. H., and W. H. Schlesinger. 1985. Forest ecosystems. Academic Press, San Diego, California, USA.